Explicit versus Implicit Solvation Effects on the First Hyperpolarizability of an Organic Biphotochrome

ARTICLE *in* THE JOURNAL OF PHYSICAL CHEMISTRY A · MARCH 2015

Impact Factor: 2.69 · DOI: 10.1021/acs.jpca.5b00631 · Source: PubMed

4 AUTHORS:

Jean Quertinmont
University of Namur
2 PUBLICATIONS **2** CITATIONS
SEE PROFILE

Benoît Champagne
University of Namur
401 PUBLICATIONS **8,753** CITATIONS
SEE PROFILE

Frédéric Castet
Université of Bordeaux
90 PUBLICATIONS **1,694** CITATIONS
SEE PROFILE

Marcelo Hidalgo Cardenuto
University of Namur
5 PUBLICATIONS **5** CITATIONS
SEE PROFILE

THE JOURNAL OF PHYSICAL CHEMISTRY A

Article

pubs.acs.org/JPCA

Explicit versus Implicit Solvation Effects on the First Hyperpolarizability of an Organic Biphotochrome

Jean Quertinmont,[†] Benoît Champagne,*[,†] Frédéric Castet,[‡] and Marcelo Hidalgo Cardenuto[†,§]

[†]Laboratoire de Chimie Théorique, Unité de Chimie Physique Théorique et Structurale, University of Namur, rue de Bruxelles, 61, B-5000 Namur, Belgium

[‡]Institut des Sciences Moléculaires (ISM), Université de Bordeaux, UMR 5255 CNRS, Cours de la Libération 351, F-33405 Talence Cedex, France

[§]Instituto de Física, Universidade de São Paulo, CP 66318, 05314-970 São Paulo, SP, Brazil

Supporting Information

ABSTRACT: The first hyperpolarizability of the four trans forms of a dithienylethene indolinooxazolidine biphotochrome in acetonitrile solution has been evaluated by using two solvation models, an explicit and an implicit one. The implicit solvation model is the integral equation formalism of the polarizable continuum model (IEF-PCM), whereas in the explicit one, the solvent molecules are represented by point charges, of which the positions have been generated by Monte Carlo simulations whereas the solute is treated quantum mechanically. At optical frequencies, first hyperpolarizabilities calculated with the implicit solvation model are usually larger than those obtained with the multiscale approach. However, both approaches predict similar contrasts, indicating that implicit solvation models such as IEF-PCM are well-suited to describe the variations in the NLO responses of molecular switches. In addition, the analysis of the contrasts of first hyperpolarizabilities shows that the biphotochrome can act as a three-state NLO switch.

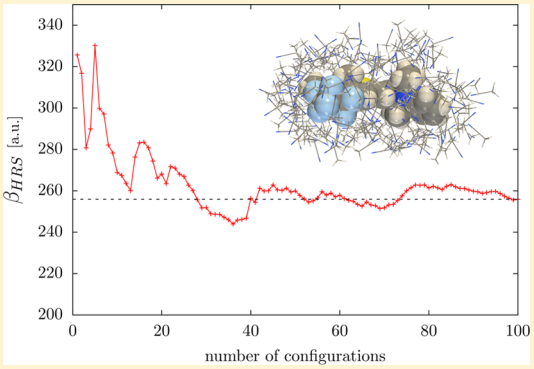

1. INTRODUCTION

Molecular properties are impacted by solvation, and the magnitude of these effects depends on the solvent characteristics but also on the nature of these properties.[1,2] Among those, nonlinear optical (NLO) properties can be strongly modified by the solvent, both owing to specific solute−solvent interactions and to electrostatic effects. This was early recognized when comparing hyperpolarizability values (β and γ, the first and the second hyperpolarizabilities, the molecular properties at the origin of second- and third-order NLO phenomena) deduced from measurements carried out in different solvents.[3] These effects have also generated a lot of theoretical studies, accompanied by the elaboration of models implemented at different levels of approximation to rationalize these effects. In this field, Tomasi and co-workers have pioneered the development of methods based on the polarizable continuum model (PCM), involving also the description of weak interactions and local field effects.[4−8] Over the last two decades, theoretical and computational studies have addressed, for example, (i) the different levels of approximation used to describe the self-consistent reaction field and the polarizable continuum model,[9−12] (ii) the relationship between the nature of the solute and solvent and the magnitude of solvent effects on the solute hyperpolarizabilities,[13−18] (iii) the interplay between geometrical structures, linear and nonlinear optical responses of push−pull π-conjugated systems, and the dielectric constant of the solvent,[19,20] (iv) the use of methods combining quantum mechanics and molecular mechanics (QM/MM),[20−22] (v) the dual impact of solvent on the first hyperpolarizability contrast of molecular switches,[23] and (vi) the effects of solute concentration.[24−27]

This paper deals with the description of solvent effects on the first hyperpolarizability β of a biphotochrome (Figure 1) and, in particular, with the comparison of results obtained with two types of methods, (i) a QM/MM scheme where the explicit effects of the solvent are described by point charges while the spatial distributions of solute and solvent molecules are generated using Monte Carlo simulations and (ii) the PCM approach where the solvent effects are treated implicitly. To achieve this goal, a recently synthesized dithienylethene indolinooxazolidine biphotochrome has been selected.[28,29] This biphotochrome has been shown to act as an octastate switch displaying distinct UV/vis absorption spectra. The details of the acido-, photo-, and thermo-induced chemical transformations have been unraveled by NMR spectroscopy.

Special Issue: Jacopo Tomasi Festschrift

Received: January 21, 2015
Revised: March 6, 2015
Published: March 9, 2015

DOI: 10.1021/acs.jpca.5b00631
J. Phys. Chem. A 2015, 119, 5496−5503

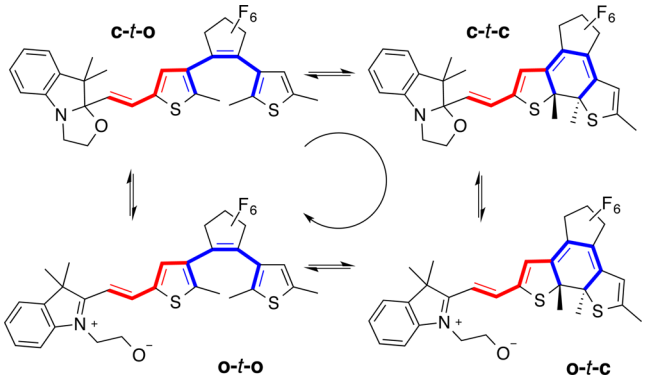

Figure 1. Equilibria between the four trans forms of the dithienylethene indolinooxazolidine biphotochrome. The red bonds define the common π-conjugated segment and the blue ones the two torsion angles of the dithienylethene moiety. The acronyms of the different isomers are also given.

Here, the quartet of trans isomers, which are more stable than the cis forms, is considered (Figure 1).

The calculations of the solvent effects do not only focus on the amplitude of the biphotochrome β but also on the β contrasts between the different isomers, since this is a key quantity to design multistate, multifunctional, and multi-triggered molecular switches.[30,31] The paper is organized as follows: (i) Section 2 provides a summary of the theoretical approaches and computational schemes, (ii) Section 3 presents the results and gives interpretations, and (iii) conclusions are drawn in Section 4.

2. COMPUTATIONAL PROCEDURES

The geometries of the four isomers of the biphotochrome were optimized at the density functional theory (DFT) level using the M06 exchange-correlation (XC) functional[32] and the 6-311G* basis set. To take into account the effects of the solvent on the geometries, the optimizations were carried out within the integral equation formalism of PCM (IEF-PCM), with acetonitrile as the solvent. On the other hand, the solvent effects on the NLO properties of the biphotochrome are described with both an explicit and an implicit scheme, more precisely, (i) using a hybrid method that combines MM simulations with QM calculations and (ii) the IEF-PCM scheme, respectively. In both cases, the solvent is acetonitrile.

In the explicit method, a sequential QM/MM (S-QMMM) approach[33−38] was adopted. First, classical Monte Carlo (MC) simulations are performed to generate the structure of the liquid environment (configurations or snapshots) around the target biphotochrome. Then, these configurations are used in QM calculations to obtain the NLO properties. The thermodynamic conditions used in the simulations are T = 298.15 K and a density ρ of 0.777 g/cm^3 in the NVT ensemble. Using these conditions, the configurations of the biphotochrome and a total of 1500 acetonitrile molecules were simulated in a cubic box with periodic boundary conditions.[39] These were carried out for each of the four forms of the biphotochrome. Their geometries were kept frozen and those of the acetonitrile as well. In the MC simulations, the intermolecular interactions were described by both a Lennard-Jones potential and a Coulomb electrostatic potential term. The atomic charges of the biphotochrome (needed for the Coulomb part of the potential) were determined using the CHELPG procedure[40] at the M06/6-311G* level. The Lennard-Jones parameters were taken from the OPLS (optimized potential for liquid simulations) force field. For the acetonitrile molecules, the force field for liquid acetonitrile described in ref 41 was selected. All MC simulations were performed using the DICE program.[42] In order to provide information about the solvation shells around the biphotochrome, the minimum-distance distribution function (MDDF)[43] was calculated. Owing to the elongated shape of the biphotochrome, the MDDF is preferred over the more traditional radial distribution function that considers the distances between the molecule centers of mass. These MC simulations provide a set of configurations containing the target molecule embedded in the solvent environment. The energy autocorrelation function[44,45] is used to evaluate the interval of correlation (i.e., the interval necessary to obtain statistically uncorrelated configurations). To calculate the NLO properties, the solvent is described by point charges (PC). Indeed, calculating routinely at a full QM level, the molecular properties for the whole systems (the solute and the 1500 solvent molecules represent a total of 9067 atoms) is still prohibitive with current computational resources. Thus, the biphotochrome is surrounded by an electrostatic embedding composed by the PC of which the positions were generated in the MC simulations. The NLO properties (static and dynamic β) are obtained at the coupled-perturbed Hartree−Fock (CPHF) and time-dependent Hartree−Fock (TDHF) levels,[47,48] using the 6-311+G* basis set. Though electron correlation effects could have been accounted for by resorting to DFT with range-separated XC functionals, their advantage over the HF level for push−pull π-conjugated systems is still a matter of debate,[49−51] whereas high-level ab initio treatments are still computationally prohibitive. To investigate the effects of the outer solvation shells, successive calculations were performed by considering increasing numbers of shells, from the first one to the limits of the box.

In the implicit method, the same properties were calculated at the same CPHF and TDHF levels of approximation, using the 6-311+G* basis set. In the IEF-PCM scheme, the solute is considered in a cavity, of which the shape is obtained by the interlocking van der Waals spheres centered at the atoms of the molecule,[46] and the solvent is characterized by its (static or dynamic) dielectric constants. The radius of these spheres is fixed to 1.1 times the United Force Field (UFF) van der Waals radius. All quantum chemistry calculations, with PC as well as with IEF-PCM, were performed using the Gaussian09 program package.[52]

The work focuses on two quantities, β_{HRS} and its depolarization ratio (DR), associated with hyper-Rayleigh scattering (HRS) experiments. β_{HRS} is proportional to the intensity of the vertically polarized (along the Z axis) signal scattered at 90° with respect to the propagation direction (Y axis) for a nonpolarized incident light. DR, which depends on the NLOphore shape, is the ratio between the scattered intensities obtained when the incident light is vertically ($\langle\beta^2_{ZZZ}\rangle$) and horizontally ($\langle\beta^2_{ZXX}\rangle$) polarized:

$$DR = \frac{\langle\beta^2_{ZZZ}\rangle}{\langle\beta^2_{ZXX}\rangle}$$

with

$$\langle\beta^2_{HRS}\rangle = \langle\beta^2_{ZZZ}\rangle + \langle\beta^2_{ZXX}\rangle$$

DOI: 10.1021/acs.jpca.5b00631
J. Phys. Chem. A 2015, 119, 5496−5503

Detailed expressions of the orientational averages $\langle \beta^2_{ZZZ} \rangle$ and $\langle \beta^2_{ZXX} \rangle$ as a function of the β tensor components in the molecular frame are available in ref 17. All reported β values are in atomic units (1 au of $\beta = 3.6310^{-42}$ m^4 $V^{-1} = 3.2063 \times 10^{-53}$ C^3 m^3 $J^{-2} = 8.641 \times 10^{-33}$ esu) within the T convention.

3. RESULTS AND DISCUSSION

A first simulation step, called thermalization, was carried out to stabilize the system (1.2×10^5 steps) then the actual simulation runs 3×10^5 steps for which the atomic coordinates of every hundredth step are saved. Using these configurations, the MDDFs are calculated and then normalized to define the two first solvation shells and the number of acetonitrile molecules in these shells. The third shell was fixed at 15.05 Å, defining the zone where the solvent is structured around the solute, and the fourth one is determined by the box containing all the 1500 acetonitrile molecules. Table 1 gives the characteristics of each shell, and Figure 2 the MDDF for **c-*t*-c** (see the Supporting Information for the other forms).

Table 1. Characteristics of the Successive Solvation Shells[a]

		shell 1	shells 1−2	shells 1−3	shells 1−4
c-*t*-o	*r*	4.05	7.85	15.05	—
	s	40	126	471	1500
c-*t*-c	*r*	4.05	8.05	15.05	—
	s	39	130	466	1500
o-*t*-c	*r*	4.05	8.15	15.05	—
	s	41	135	468	1500
o-*t*-o	*r*	4.05	8.25	15.05	—
	s	41	139	473	1500

[a] *r* (Å) is the minimal distance, and *s* the number of solvent molecules.

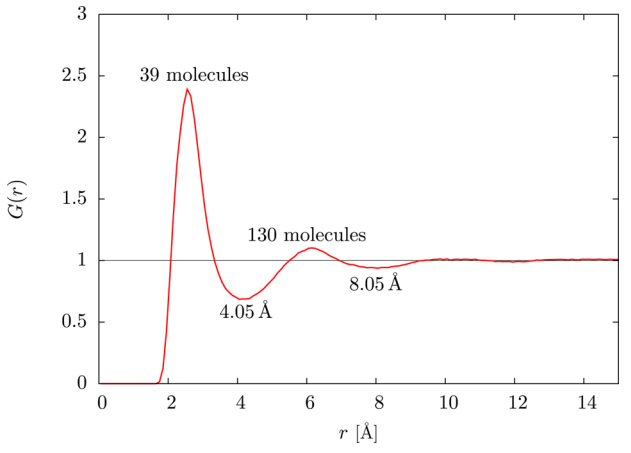

Figure 2. Normalized minimal distance distribution function for **c-*t*-c** in acetonitrile.

The energy autocorrelation functions (Figure 3 for **c-*t*-c** and the Supporting Information for the other forms) were fitted with a sum of two exponential functions to get the correlation steps, as well as 2τ (Table S1 in the Supporting Information), the minimum number of steps between two configurations to ensure they are uncorrelated. This condition has to be fulfilled for applying statistics to get the system properties. In all cases, uncorrelated configurations are obtained after at most 227 steps. To achieve a statistical convergence of the molecular properties, 100 configurations were selected. This corresponds to one configuration every 3000 steps, well above the 2τ values,

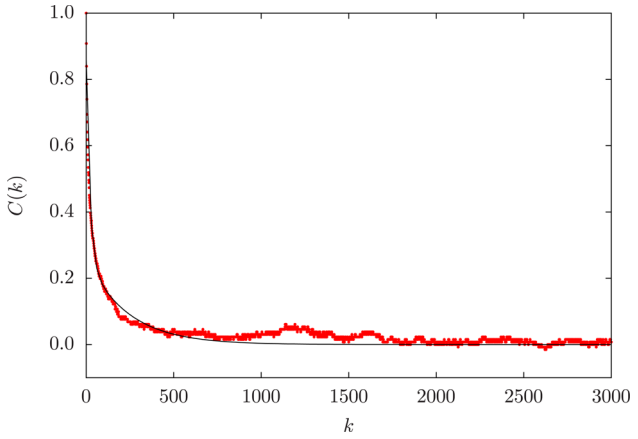

Figure 3. Energy autocorrelation function for **c-*t*-c** in acetonitrile (k is the number of steps separating two configurations).

corresponding to an almost zero value for the energy autocorrelation function.

Figure 4 describes the evolution of the average β_{HRS} and DR for **c-*t*-c** (for the other forms, see the Supporting Information)

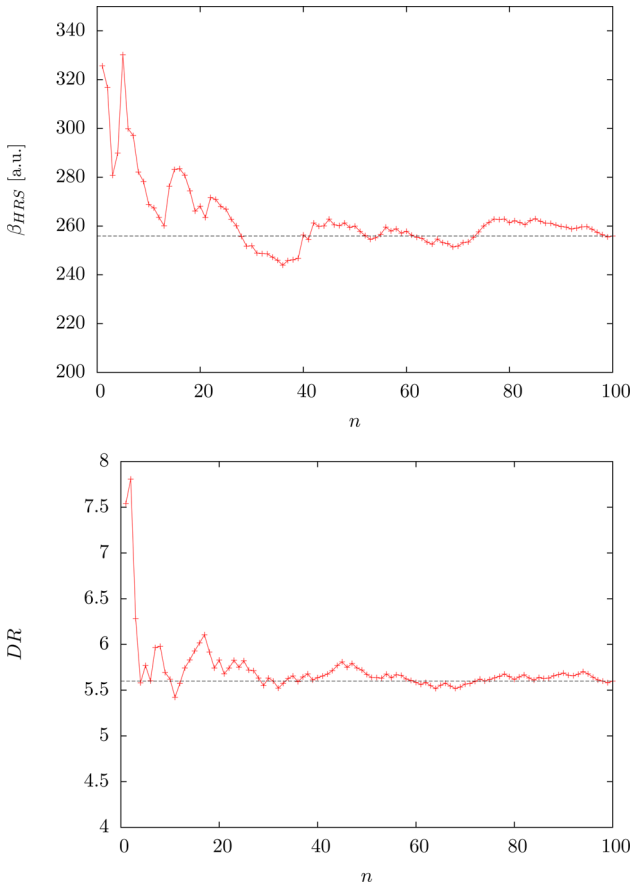

Figure 4. CPHF/6-311+G* β_{HRS} (top) and DR (bottom) of **c-*t*-c** as a function of the number of configurations n (using 1500 solvent molecules).

as a function of the number of configurations n (using 1500 solvent molecules represented by PC). Rapid convergence is achieved for both properties and for all forms. Then, the effect of the number of solvation shells or of the number of solvent molecules surrounding the solute, s, on the NLO properties was

DOI: 10.1021/acs.jpca.5b00631
J. Phys. Chem. A 2015, 119, 5496−5503

studied. The static β_{HRS} and DR were computed by adding up to four solvation shells. The average values and standard deviations for a hundred configurations (n = 100) are given in Table 2 for **c-*t*-c**. The β_{HRS} values decrease with s, highlighting

Table 2. CPHF/6-311+G* β_{HRS} and DR of the c-*t*-c Form As a Function of the Number of Solvent Molecules s (Using 100 Configurations to Evaluate the Averages) And Their Respective Standard Deviations σ

	shell 1	shells 1−2	shells 1−3	shells 1−4
s	39	130	466	1500
β_{HRS} (a.u.)	287.8	270.9	265.5	255.9
σ	128.9	132.6	110.5	98.1
DR	5.57	5.52	5.57	5.60
σ	1.75	1.87	1.92	1.90

the polarization effects of the surrounding shells. On the other hand, DR is almost constant with s. The β_{HRS} standard deviation σ decreases with s (provided the number of shells is at least 2), whereas for DR, it slightly increases. These calculations indicate that long-range electrostatic effects (i.e., beyond the first solvation shell) have a non-negligible impact on the NLO responses of the solute molecules. On this basis, the following calculations were performed by using 100 configurations with the full set of 1500 solvent molecules (the CPU time is almost independent of the number of PC).

3.1. Static Responses. The average static β_{HRS} and DR are listed in Table 3. The β_{HRS} amplitudes are ordered according to

$$\textbf{o-}t\textbf{-c} > \textbf{o-}t\textbf{-o} > \textbf{c-}t\textbf{-o} \sim \textbf{c-}t\textbf{-c} \quad (1)$$

Table 3. CPHF/6-311+G* Static β_{HRS} and DR (and Their Standard Deviations) of the Trans Forms of the Biphotochrome (Averaged over 100 Configurations) As-Determined within the Surrounding Polarization Field of 1500 Acetonitrile Molecules Represented As Point-Charges in Comparison to the BLA of the π-Conjugated Segment and the Average Torsion Angles of the Dithienylethene Moiety

	c-*t*-o	c-*t*-c	o-*t*-c	o-*t*-o
β_{HRS}	280.7	255.9	5300.4	1869.2
σ (%)	20.4	38.3	22.9	14.5
DR	6.67	5.60	4.16	3.85
σ (%)	9.4	33.9	5.0	4.9
BLA (Å)	0.085	0.083	0.050	0.054
torsion angle (deg)	45.0	7.6	8.4	45.3

This demonstrates the dominant β contribution of the indolinooxazolidine moiety in its open form. The dithienylethene fragment has a smaller contribution to the global β response. However, when closed, it further contributes to enhance the first hyperpolarizability of the compound by extending the π-conjugation along the whole system. The β_{HRS} ordering can be analyzed by considering geometrical parameters such as the bond length alternation (BLA) of the π-conjugated segment or the torsion angles of the dithienylethene moiety (Figure 1, Table 3). Indeed, the smallest BLA values, characterizing the open indolinooxazolidine moiety, are associated with the largest β_{HRS}, which is further exalted when the dithienylethene moiety is closed (i.e., when its average torsion angle is close to planarity).

The standard deviations, which measure the dispersion from the average values and highlight the impact of the solvent configurations, are of similar amplitude, except in the case of the **c-*t*-c** isomer with 38% of dispersion for β_{HRS} and 34% for DR. In order to trace the origin of the large broadening in the β_{HRS} responses for this isomer, the configurations giving β_{HRS} values larger than 400 au were superimposed and the same was done for those associated with values smaller than 150 au (Figure 5). It is observed that the presence of acetonitrile

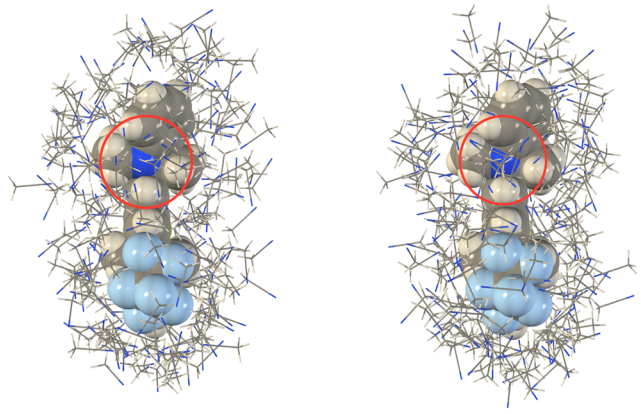

(a) β_{HRS} larger than 400 a.u.. (b) β_{HRS} smaller than 150 a.u..

Figure 5. Superimposition of 7 configurations of **c-*t*-c** selected on the basis of the β_{HRS} amplitude. **c-*t*-c** is represented using atomic van der Waals spheres, while only the first solvent shell is shown, using sticks representation.

molecules on top of the nitrogen leads to smaller β_{HRS} values. Since the Mulliken charge on the N atom is negligibly impacted by the presence of these acetonitrile molecules, the effect on β_{HRS} has an electrostatic origin.

3.2. Dynamic Responses. The average dynamic β_{HRS} and DR are given in Table 4, with their standard deviations. Overall,

Table 4. TDHF/6-311+G* Dynamic β_{HRS} and DR (and Their Standard Deviations) for the Different Forms of the Biphotochrome (Averaged Over 100 Configurations, within the Explicit Solvation Model with 1500 Acetonitrile Molecules Represented by Point Charges)

λ (nm)		c-*t*-o	c-*t*-c	o-*t*-c	o-*t*-o
1907	β_{HRS}	300.3	301.9	8036.4	2160.8
	σ (%)	20.8	44.0	23.7	15.3
	DR	6.65	5.98	4.38	3.91
	σ (%)	9.8	32.6	4.1	5.1
1064	β_{HRS}	355.6	613.7	83736.8	3232.3
	σ (%)	21.8	57.9	55.6	17.6
	DR	6.56	5.68	4.98	4.02
	σ (%)	10.5	26.1	1.2	6.0

the dynamic β_{HRS} are larger than the static ones, the responses at 1064 nm being, as expected, the largest, while the relative ordering of the β_{HRS} values of the four isomers remains unchanged. However, if at 1907 nm, the **c-*t*-c** and **c-*t*-o** isomers have similar β_{HRS} responses, at 1064 nm, the **c-*t*-c** isomer displays a β_{HRS} value that is about twice that of **c-*t*-o**. This enhancement comes from the dithienylethene moiety. When the indolinooxazolidine moiety is closed, the molecule does not contain any strong NLOphore, and the static β_{HRS} response is small. Still, at smaller wavelength, resonance enhancements occur and they are facilitated by the closed dithienylethene

DOI: 10.1021/acs.jpca.5b00631
J. Phys. Chem. A 2015, 119, 5496−5503

form. The magnitude of these resonance enhancements is consistent with the excitation wavelength of the dipole-allowed excited state that dominates the UV/vis absorption spectra (TDHF/6-311+G* λ = 272, 427, 528, and 362 nm for **c-*t*-o**, **c-*t*-c**, **o-*t*-c**, and **o-*t*-o**, respectively).

The standard deviations are of the same order of magnitude at 1907 nm as in the static case. At 1064 nm, σ of β_{HRS} of the **c-*t*-c** and **o-*t*-c** forms increases to 58% and 56%, respectively. In the case of **o-*t*-c**, some geometrical configurations favor slightly resonant conditions that also contribute to broaden the β_{HRS} distribution with respect to the static case (see Figure 6). The static and dynamic depolarization ratios are similar.

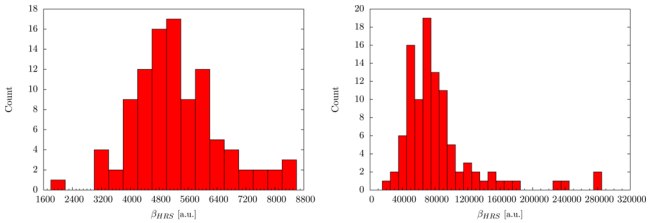

(a) Static (width = 400 a.u.). (b) 1064 nm (width = 10000 a.u.).

Figure 6. Distribution of the static and dynamic (λ = 1064 nm) β_{HRS} responses for the **o-*t*-c** form.

4. IMPLICIT SOLVATION AND COMPARISON WITH THE EXPLICIT SOLVATION RESULTS

Table 5 lists the β_{HRS} and DR values calculated using the implicit (IEF-PCM) method, with acetonitrile as the solvent.

Table 5. IEF-PCM/TDHF/6-311+G* Static and Dynamic β_{HRS} and DR of the Four Biphotochrome Isomers in Acetonitrile Solution

λ (nm)		**c-*t*-o**	**c-*t*-c**	**o-*t*-c**	**o-*t*-o**
∞	β_{HRS}	505.2	511.8	14886.5	3806.9
	DR	6.21	8.13	4.39	3.82
1907	β_{HRS}	376.9	265.5	12883.2	3013.6
	DR	6.77	8.38	4.66	4.18
1064	β_{HRS}	451.5	600.7	—	4752.0
	DR	6.74	7.02	—	4.37

Since the static dielectric constant of acetonitrile (ϵ_0 = 35.69) is larger than the dynamic one (ϵ_∞ = 1.81), the static β_{HRS} values are larger than those calculated at 1907 and 1064 nm. Due to the large ϵ_0 value used in the IEF-PCM scheme, the implicit solvation approach gives larger static β_{HRS} than the explicit solvation scheme (from 80 to 181% larger). On the other hand, the depolarization ratios are similar, except for **c-*t*-c** (which is a poor NLOphore). Although the differences are smaller, the IEF-PCM β_{HRS} values calculated at 1907 and 1064 nm are also larger than those obtained with the PC electrostatic surrounding, except in the case of **c-*t*-c**, for which the explicit model gives slightly larger responses (by less than 14%). The DR keep the same behavior as in the static case.

The contrast ratios for the static and dynamic β_{HRS} are given in Table 6. Considering first the results obtained with the explicit solvation scheme, the (**c-*t*-o** → **c-*t*-c**) contrast ratio is close to one. Then, going from **c-*t*-c** to **o-*t*-c**, the HRS response increases substantially, with contrasts larger than 20. When opening the dithienylethene moiety to get **o-*t*-o**, the contrast is smaller than one, and, finally, β_{HRS} further decreases along the last switching process, from **o-*t*-o** to **c-*t*-o**. When going from static to dynamic responses as well as when the incident photon energy increases, the contrast ratios are exalted, getting further away from one. Note that at 1064 nm, the contrasts involving the **o-*t*-c** form are impacted by a resonance enhancement. Figure 7 summarizes the contrasts and their frequency dispersion. When turning to the implicit solvation results, the contrast ratios are similar, though the implicit contrasts are generally more pronounced (further away from one) than the explicit ones. A qualitative difference between the two solvation models is observed for the first equilibrium (**c-*t*-o** → **c-*t*-c**), where in the static case the explicit model predicts a contrast slightly smaller than 1, while using the explicit model a negligible β_{HRS} variation is predicted along the commutation. The situation is reversed at 1907 nm. At 1064 nm, both contrasts are larger than one.

Table 6. Static and Dynamic β_{HRS} Contrasts for the Four Equilibria Using IEF-PCM in Acetonitrile (Implicit) or the Average Value from a Hundred Configurations with Point Charges (Explicit) as Evaluated at the HF/6-311+G* Level

λ (nm)		**c-*t*-o** → **c-*t*-c**	**c-*t*-c** → **o-*t*-c**	**o-*t*-c** → **o-*t*-o**	**o-*t*-o** → **c-*t*-o**
∞	implicit	1.01	29.09	0.26	0.13
	explicit	0.91	20.71	0.35	0.15
1907	implicit	0.74	48.52	0.23	0.12
	explicit	1.00	26.62	0.27	0.14
1064	implicit	1.33	—	—	0.09
	explicit	1.73	136.46	0.04	0.11

5. CONCLUSIONS

The first hyperpolarizability of the four trans isomers of a dithienylethene indolinooxazolidine biphotochrome in acetonitrile solution has been evaluated by using both explicit and implicit solvation models. In the explicit one, the solvent molecules are represented by point charges, of which the positions have been generated by Monte Carlo simulations, whereas the solute is treated quantum mechanically. The implicit solvation model is the integral equation formalism of the polarizable continuum model (IEF-PCM) that has been developed by Tomasi and co-workers.[4−8] At optical frequencies, the hyper-Rayleigh scattering first hyperpolarizabilities, β_{HRS}, calculated with the implicit solvation model are usually larger than those obtained with the multiscale approach. However, both models predict similar contrasts, indicating that implicit solvation models such as IEF-PCM are well-suited to describe the variations in the NLO responses of molecular switches. Then, with the exception of **c-*t*-c**, which is a poor NLOphore, the calculated depolarization ratios are very similar to both methods. The analysis of the β_{HRS} contrasts shows that the biphotochrome can act as a three-state NLO switch. Indeed, only the β_{HRS} contrast between forms **c-*t*-o** and **c-*t*-c** is close to one, showing the small impact of opening/closing the dithienyethene part when the oxazolidine moiety is closed. On the other hand, opening the oxazolidine moiety from **c-*t*-c** to **o-*t*-c** is characterized by a contrast larger than 20, whereas the contrasts for the **o-*t*-c** to **o-*t*-o** and **o-*t*-o** to **c-*t*-o** transformations are clearly smaller than one.

DOI: 10.1021/acs.jpca.5b00631
J. Phys. Chem. A 2015, 119, 5496−5503

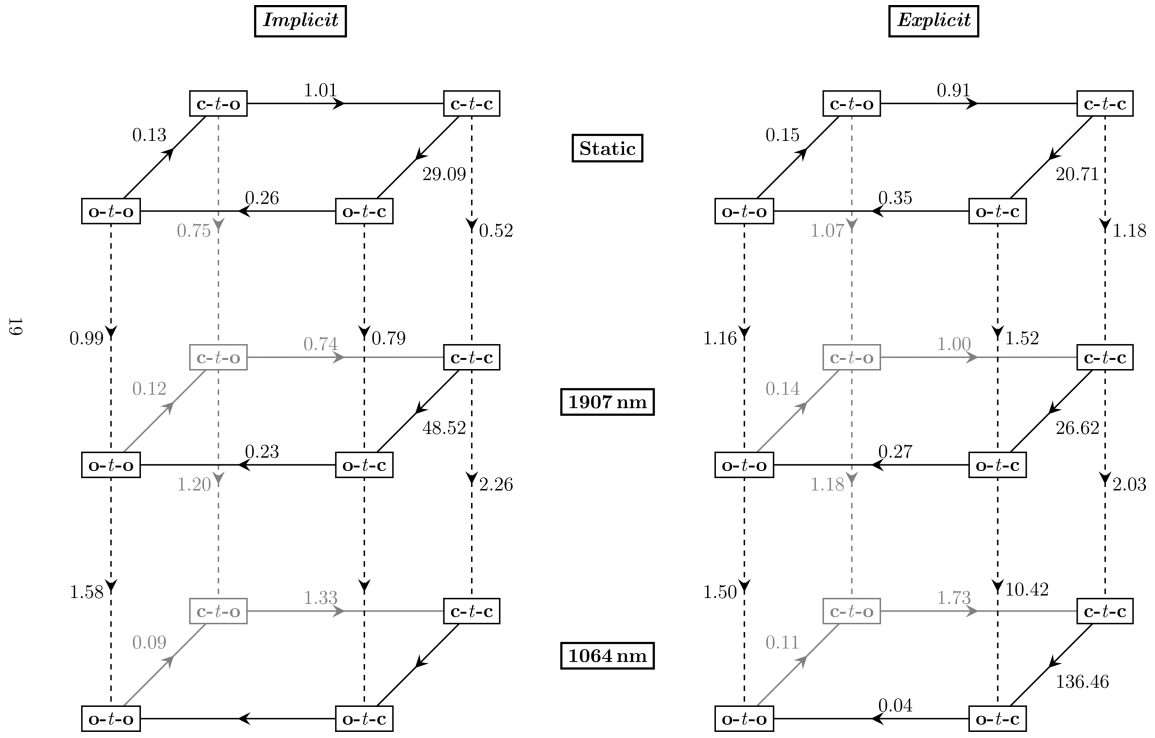

Figure 7. Implicit (left) versus explicit (right) β_{HRS} contrasts for the four switching equilibria between the trans forms of the biphotochrome as determined at the HF/6-311+G* level at different wavelengths.

■ ASSOCIATED CONTENT

Supporting Information

Normalized minimal distance distribution functions, energy autocorrelation functions, distributions of the CPHF/6-311+G* (static) and TDHF/6-311+G* (1907 nm) β_{HRS} responses for the four isomers. Parameters of the fit of the energy autocorrelation function for each isomer. This material is available free of charge via the Internet at http://pubs.acs.org.

■ AUTHOR INFORMATION

Corresponding Author

*E-mail: benoit.champagne@unamur.be.

Notes

The authors declare no competing financial interest.

■ ACKNOWLEDGMENTS

This paper is dedicated to Jacopo Tomasi for the occasion of his 80th birthday, in particular for the very many enlightening and friendly discussions one of the authors has had with him over the last 20 years. M.H.C. acknowledges the CNPq (Brazil) and University of São Paulo for his postdoctoral grant as well as the Belgian Government (IUAP No P7/5 "Functional Supramolecular Systems") for financial support. This work is supported by funds from the Belgian Government (IUAP No P7/5) and the Francqui Foundation. The calculations were performed on the computers of the Consortium des Équipements de Calcul Intensif and mostly those of the Technological Platform of High-Performance Computing, for which we gratefully acknowledge the financial support of the FNRS-FRFC (Conventions 2.4.617.07.F and 2.5020.11) and of the University of Namur.

■ REFERENCES

(1) Bishop, D. M. Effect of the Surroundings on Atomic and Molecular Properties. *Int. Rev. Phys. Chem.* **1994**, *13*, 21−39.

(2) Reichardt, C., Welton, T. *Solvents and Solvent Effects in Organic Chemistry*; Wiley VCH: Weinheim, Germany, 2011.

(3) Cheng, L. T.; Tam, W. H.; Stevenson, S. H.; Meredith, G. R.; Rikken, G.; Marder, S. R. Experimental Investigations of Organic Molecular Nonlinear Optical Polarizabilities. 1. Methods and Results on Benzene and Stilbene Derivatives. *J. Phys. Chem.* **1991**, *95*, 10631−10643.

(4) Cammi, R.; Cossi, M.; Tomasi, J. Analytical Derivatives for Molecular Solutes. III. Hartree-Fock Static Polarizability and Hyperpolarizabilities in the Polarizable Continuum Model. *J. Chem. Phys.* **1996**, *104*, 4611.

(5) Cammi, R.; Cossi, M.; Tomasi, J. Analytical Hartree-Fock Calculation of the Dynamical Polarizabilities α, β and γ of Molecules in Solution. *J. Chem. Phys.* **1996**, *105*, 10556.

(6) Cammi, R.; Mennucci, B.; Tomasi, J. Solvent Effects on Linear and Nonlinear Optical Properties of Donor-Acceptor Polyenes: Investigation of Electronic and Vibrational Components in Terms of Structure and Charge Distribution Changes. *J. Am. Chem. Soc.* **1998**, *120*, 8834−8847.

(7) Mennucci, B.; Amovilli, C.; Tomasi, J. On the Effect of Pauli Repulsion and Dispersion on Static Molecular Polarizabilities and Hyperpolarizabilities in Solution. *Chem. Phys. Lett.* **1998**, *286*, 221−225.

(8) Cammi, R.; Frediani, L.; Mennucci, B.; Tomasi, J. Calculation of Nonlinear Optical Susceptibilities of Pure Liquids Within the Polarizable Continuum Model: the Effect of the Macroscopic Nonlinear Polarization at the Output Frequency. *J. Mol. Struct. (THEOCHEM)* **2003**, *633*, 209−216.

(9) Yu, J.; Zerner, M. C. Solvent Effect on the First Hyperpolarizabilities of Conjugated Organic Molecules. *J. Chem. Phys.* **1994**, *100*, 7487.

(10) Mikkelsen, K. V.; Luo, Y.; Ågren, H.; Jørgensen, P. Solvent Induced Polarizabilities and Hyperpolarizabilities of para-nitroaniline

DOI: 10.1021/acs.jpca.5b00631
J. Phys. Chem. A 2015, 119, 5496−5503

Studied by Reaction Field Linear Response Theory. *J. Chem. Phys.* **1994**, *100*, 8240.
(11) Di Bella, S.; Marks, T. J.; Ratner, M. A. Environmental Effects on Nonlinear Optical Chromophore Performance. Calculation of Molecular Quadratic Hyperpolarizabilities in Solvating Media. *J. Am. Chem. Soc.* **1994**, *116*, 4440−4445.
(12) Cammi, R. Coupled-cluster Theory for the Polarizable Continuum Model. III. A Response Theory for Molecules in Solution. *Int. J. Quantum Chem.* **2012**, *112*, 2547−2560.
(13) Ferrighi, L.; Frediani, L.; Cappelli, C.; Salek, P.; Ågren, H.; Helgaker, T.; Ruud, K. Density-Functional-Theory Study of the Electric-Field-Induced Second Harmonic Generation (EFISHG) of Push-Pull Phenylpolyenes in Solution. *Chem. Phys. Lett.* **2006**, *425*, 267−272.
(14) Ferrighi, L.; Frediani, L.; Ruud, K. Degenerate Four-Wave Mixing in Solution by Cubic Response Theory and the Polarizable Continuum Model. *J. Phys. Chem. B* **2007**, *111*, 8965−8973.
(15) Takimoto, Y.; Isborn, C. M.; Eichinger, B. E.; Rehr, J. J.; Robinson, B. H. Frequency and Solvent Dependence of Nonlinear Optical Properties of Molecules. *J. Phys. Chem. C* **2008**, *112*, 8016−8021.
(16) Lu, S. I.; Chiu, C. C.; Wang, Y. F. Density Functional Theory Calculations of Dynamic First Hyperpolarizabilities for Organic Molecules in Organic Solvent: Comparison to Experiment. *J. Chem. Phys.* **2011**, *135*, 134104.
(17) Castet, F.; Bogdan, E.; Plaquet, A.; Ducasse, L.; Champagne, B.; Rodriguez, V. Reference Molecules for Nonlinear Optics: A Joint Experimental and Theoretical Investigation. *J. Chem. Phys.* **2012**, *136*, 024506.
(18) Wergifosse, M.; Ruyck, J.; Champagne, B. How the Second-Order Nonlinear Optical Response of the Collagen Triple Helix Appears: A Theoretical Investigation. *J. Phys. Chem. C* **2014**, *118*, 8595−8602.
(19) Dehu, C.; Meyers, F.; Hendrickx, E.; Clays, K.; Persoons, A.; Marder, S. A.; Brédas, J. L. Solvent Effects on the Second-Order Nonlinear Optical Response of π-Conjugated Molecules: A Combined Evaluation through Self-Consistent Reaction Field Calculations and Hyper-Rayleigh Scattering Measurements. *J. Am. Chem. Soc.* **1995**, *117*, 10127−10128.
(20) Murugan, N. A.; Kongsted, J.; Rinkevicius, Z.; Ågren, H. Breakdown of the First Hyperpolarizability/Bond-Length Alternation Parameter Relationship. *Proc. Natl. Acad. Sci. U.S.A.* **2010**, *107*, 16453−16458.
(21) Kongsted, J.; Anders, A.; Mikkelsen, K. V.; Christiansen, O. Second Harmonic Generation Second Hyperpolarizability of Water Calculated Using the Combined Coupled Cluster Dielectric Continuum or Different Molecular Mechanics Methods. *J. Chem. Phys.* **2004**, *120*, 3787.
(22) Nielsen, C. B.; Christiansen, O.; Mikkelsen, K. V.; Kongsted, J. Density Functional Self-consistent Quantum Mechanics/Molecular Mechanics Theory for Linear and Nonlinear Molecular Properties: Applications to Solvated Water and Formaldehyde. *J. Chem. Phys.* **2007**, *126*, 154112.
(23) Bogdan, E.; Plaquet, A.; Antonov, L.; Rodriguez, V.; Ducasse, L.; Champagne, B.; Castet, F. Solvent Effects on the Second-Order Nonlinear Optical Responses in the Keto-Enol Equilibrium of a 2-Hydroxy-1-naphthaldehyde Derivative. *J. Phys. Chem. C* **2010**, *114*, 12760−12768.
(24) Chen, J.; Wong, K. Y. Study of Intermolecular Interactions in Liquid Nitrobenzene by Depolarized Hyper-Rayleigh Scattering. *J. Chem. Phys.* **2005**, *122*, 174505.
(25) Shelton, D. P. Nonlocal Hyper-Rayleigh Scattering From Liquid Nitrobenzene. *J. Chem. Phys.* **2010**, *132*, 154506.
(26) Shelton, D. P. Long Range Dipole-Dipole Correlations in Nitrobenzene-Benzene Solutions. *J. Chem. Phys.* **2010**, *133*, 234507.
(27) Hidalgo Cardenuto, M.; Champagne, B. QM/MM Investigation of the Concentration Effects on the Second-Order Nonlinear Optical Responses of Solutions. *J. Chem. Phys.* **2014**, *141*, 234104.
(28) Sevez, G.; Gan, J.; Delbaere, S.; Vermeersch, G.; Sanguinet, L.; Levillain, E.; Pozzo, J. L. Photochromic Performance of a Dithienylethene-indolinooxazolidine Hybrid. *Photochem. Photobiol. Sci.* **2010**, *9*, 131−135.
(29) Szalóki, G.; Sevez, G.; Berthet, J.; Pozzo, J. L.; Delbaere, S. A Simple Molecule-Based Octastate Switch. *J. Am. Chem. Soc.* **2014**, *136*, 13510−13513.
(30) Castet, F.; Rodriguez, V.; Pozzo, J. L.; Ducasse, L.; Plaquet, A.; Champagne, B. Design and Characterization of Molecular Nonlinear Optical Switches. *Acc. Chem. Res.* **2013**, *46*, 2656−2665.
(31) Castet, F.; Champagne, B.; Pina, F.; Rodriguez, V. A Multistate pH-Triggered Nonlinear Optical Switch. *ChemPhysChem* **2014**, *15*, 2221−2224.
(32) Zhao, Y.; Truhlar, D. G. The M06 Suite of Density Functionals for Main Group Thermochemistry, Thermochemical Kinetics, Noncovalent Interactions, Excited States, and Transition Elements: Two New Functionals and Systematic Testing of Four M06-class Functionals and 12 Other Functionals. *Theor. Chem. Acc.* **2008**, *120*, 215−241.
(33) Coutinho, K.; Canuto, S. Solvent Effects From a Sequential Monte Carlo-Quantum Mechanical Approach. *Adv. Quantum Chem.* **1997**, *28*, 89−105.
(34) Coutinho, K.; Canuto, S.; Zerner, M. C. Calculation of the Absorption Spectrum of Benzene in Condensed Phase. A Study of The Solvent Effects. *Int. J. Quantum Chem.* **1997**, *65*, 885−891.
(35) Rocha, W. R.; Coutinho, K.; Almeida, W. B.; Canuto, S. An Efficient Quantum Mechanical/Molecular Mechanics Monte Carlo Simulation of Liquid Water. *Chem. Phys. Lett.* **2001**, *335*, 127−133.
(36) Coutinho, K.; Canuto, S. Solvent Effects in Emission Spectroscopy: A Monte Carlo Quantum Mechanics Study of the $n \leftarrow \pi^*$ Shift of Formaldehyde in Water. *J. Chem. Phys.* **2000**, *113*, 9132.
(37) Hidalgo, M.; Canuto, S. A Theoretical Study of the Spectral Shifts of Xe Atom in Ar Environment. *Phys. Lett. A* **2013**, *377*, 1720−1724.
(38) Canuto, S. *Solvation Effects in Molecules and Biomolecules: Computational Methods and Applications*; Springer: New York City, 2008.
(39) Allen, M. P., Tildesley, D. J. *Computer Simulation of Liquids*. Clarendon Press: Oxford, 1987.
(40) Breneman, C. M.; Wiberg, K. B. Determining Atom-centered Monopoles From Molecular Electrostatic Potentials. The Need For High Sampling Density in Formamide Conformational Analysis. *J. Comput. Chem.* **1990**, *11*, 361−373.
(41) Böhm, H.; McDonald, I. R.; Madden, P. A. An Effective Pair Potential for Liquid Acetonitrile. *Mol. Phys.* **1983**, *49*, 347−360.
(42) Coutinho, K., Canuto, S. *DICE* (version 2.9): A General Monte Carlo Program for Liquid Simulation; University of São Paulo: São Paulo, Brazil, 2009.
(43) Georg, H. C.; Coutinho, K.; Canuto, S. Solvent Effects on the UV-Visible Absorption Spectrum of Benzophenone in Water: A Combined Monte Carlo Quantum Mechanics Study Including Solute Polarization. *J. Chem. Phys.* **2007**, *126*, 034507.
(44) Coutinho, K.; Oliveira, M. J.; Canuto, S. Sampling Configurations in Monte Carlo Simulations for Quantum Mechanical Studies of Solvent Effects. *Int. J. Quantum Chem.* **1998**, *66*, 249−253.
(45) Coutinho, K.; Canuto, S.; Zerner, M. C. A Monte Carlo-Quantum Mechanics Study of the Solvatochromic Shifts of the Lowest Transition of Benzene. *J. Chem. Phys.* **2000**, *112*, 9874.
(46) Tomasi, J. Thirty Years of Continuum Solvation Chemistry: A Review, and Prospects for the Near Future. *Theor. Chem. Acc.* **2004**, *112*, 184−203.
(47) Sekino, H.; Bartlett, R. J. Frequency Dependent Nonlinear Optical Properties of Molecules. *J. Chem. Phys.* **1986**, *85*, 976.
(48) Karna, S. P.; Dupuis, M. Frequency Dependent Nonlinear Optical Properties of Molecules: Formulation and Implementation in the HONDO Program. *J. Comput. Chem.* **1991**, *12*, 487−504.
(49) Wergifosse, M.; Champagne, B. Electron Correlation Effects on the First Hyperpolarizability of push-pull π-conjugated Systems. *J. Chem. Phys.* **2011**, *134*, 074113.

DOI: 10.1021/acs.jpca.5b00631
J. Phys. Chem. A 2015, 119, 5496−5503

(50) Garrett, K.; Sosa Vazquez, X. A.; Egri, S. B.; Wilmer, J.; Johnson, L. E.; Robinson, B. H.; Isborn, C. M. Optimum Exchange for Calculation of Excitation Energies and Hyperpolarizabilities of Organic Electro-optic Chromophores. *J. Chem. Theory Comput.* **2014**, *10*, 3821−3831.
(51) Garza, A. J.; Wazzan, N. A.; Asiri, A. M.; Scuseria, G. E. Can Short- and Middle-Range Hybrids Describe the Hyperpolarizabilities of Long-Range Charge-Transfer Compounds? *J. Phys. Chem. A* **2014**, *118*, 11787−11796.
(52) Frisch, M. J., Trucks, G. W., Schlegel, H. B., Scuseria, G. E., Robb, M. A., Cheeseman, J. R., Montgomery, J. A., Vreven, T., Kudin, K. N., Burant, J. C. et al. *Gaussian 09*, revision D01; Gaussian, Inc.: Wallingford CT, 2009.

DOI: 10.1021/acs.jpca.5b00631
J. Phys. Chem. A 2015, 119, 5496−5503